MRI Detection of Small Calcium Crystals in Air Bubble-free Agarose Phantoms: Potential Applications to Imaging Microcalcifications in Breast Cancer

B. E. Peng[1], S. Foxley[2], J. Palgen[1], R. Holmes[2], E. Hipp[2], G. Newstead[2], G. S. Karczmar[2], and D. Mustafi[1,2]
[1]Biochemistry & Molecular Biology, The University of Chicago, Chicago, Illinois, United States, [2]Radiology, The University of Chicago, Chicago, Illinois, United States

Introduction: Clusters of calcium oxalate (CaOX) and hydroxyapatite (CaHA) crystals are generally associated with benign and malignant breast lesions, respectively. Such microcalcifications (microcalcs) are useful radiological indicators of early-stage, breast carcinoma. This study tests the detectability of these microcalcs by MRI, compared to conventional x-ray imaging methods, for potential clinical applications in improved breast cancer detection. Novel air bubble-free, ultra-pure agarose phantoms were specifically developed for these MR imaging studies. Such phantoms may be easily modified for other imaging applications. Herein, MR images of microcals embedded in air bubble-free agarose phantoms were collected at high (9.4 Tesla) and at low (1.5 Tesla) field strengths, for comparison with traditional x-ray mammograms. Both calcium types were detectable and distinguishable on MR images, most likely due to unique susceptibility artifacts, while they appeared similar on x-ray mammograms.

Methods: Both individual and clustered Ca-crystals of biologically relevant size (250-500 μm) were embedded in agarose phantoms for MRI on research (9.4T) and clinical (1.5T) magnets, and for x-ray mammography. To avoid artifacts on MR images, air bubbles were removed from agarose by helium gas purge followed by overnight vacuum. High resolution MR images at 9.4T were acquired with spin echo (SE), gradient echo (GE) and echo planar spectroscopic imaging (EPSI) sequences with multiple slices of ≤500 μm in thickness and an in-plane resolution of 156 μm. MR images at 1.5T were also acquired with SE and GE sequences with multiple slices of ≤1 mm in thickness. Non-magnified clinical digital x-ray mammograms were taken with manual adjustments of kV and MAS for optimal exposure of crystals.

Results: As seen in the left panel, SE and GE images collected at 9.4T confirmed the absence of air-bubbles in homogenous, agarose phantoms, displaying only microcalcs. SE images depicted the true size of these microcalcs. GE images collected at 9.4T with a TE of 40 msec amplified the apparent crystal areas ~2.5x and ~5x for CaOX and CaHA ($p < 0.001$), respectively, due to variations in magnetic susceptibility between agarose and Ca-crystals (panel A). B_0 maps, water spectrum asymmetry and water peak height image analyses produced from sensitive EPSI datasets were used to isolate features specific to these susceptibility discontinuities, thereby localizing Ca-crystals. In the right panel, clinical GE images with TR/TE=800/10 ms of Ca-crystals embedded in various phantoms and collected at 1.5T revealed that CaHA (malignant, outlined in blue) produces larger magnetic field gradients, and therefore was more clearly visualized than CaOX (benign, outlined in green) on MR images. This distinction may aid in the detection and classification of suspicious breast lesions on MR images. In contrast, both crystal types were detectable, but not distinguishable, on x-ray mammograms.

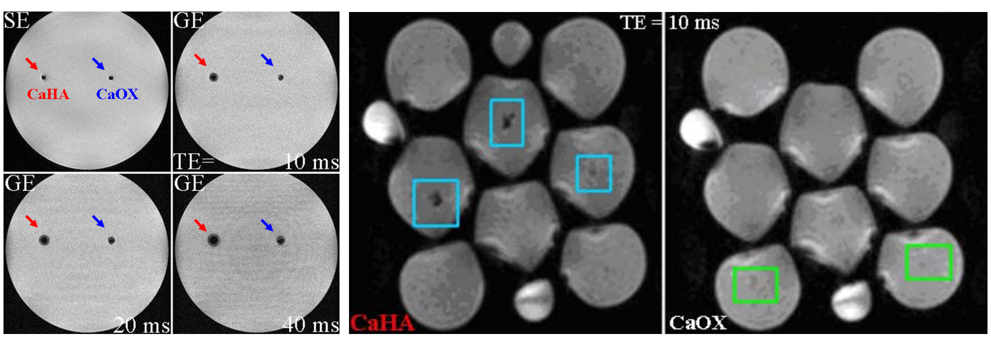

Discussion: Air bubble-free agarose phantoms allowed accurate evaluation of microcalcs on MRI at 9.4T. Such phantoms may be easily modified to mimic human tissue in terms of their relaxation pathways. For example, materials such as fat may be suspended in the agarose medium to simulate heterogeneous breast tissue. The versatility of air bubble-free agarose phantoms makes them useful tools in imaging applications. In this imaging study, Ca-crystals associated with malignant and benign lesions were distinguished at a lower field used in clinical scans; malignant-associated microcalcs produce larger magnetic susceptibility gradients and are therefore more conspicuous on T_2*-weighted MR images. Ca-crystals were clearly resolved on clinical x-ray mammograms, but could not be distinguished, suggesting the need for an alternative imaging method that can identify Ca-crystals and their associated lesion type.

Conclusion: The results presented here demonstrate that CaOX and CaHA crystals commonly associated with benign and malignant breast lesions, respectively, are clearly detectable and distinguishable by MRI in both research and clinical magnets. The present results lend support to the feasibility of clinical visualization and analysis of microcals by MRI. Detection of microcalcs by MRI would increase sensitivity and specificity for breast cancer detection.